RESEARCH ARTICLE
doi: 10.2306/scienceasia1513-1874.2022.077

ScienceAsia 48 (2022): **588–595**

Adsorption of Ni^{2+} on malic acid modified activated carbon from *Phragmites australis*

Dongmei He[a], Jian Zhang[a,*], Zhenxin Shang[b], Chenglu Zhang[b]

[a] Department of Chemical Engineering and Materials, Jining University, Shandong 273155 China
[b] Shandong Key Laboratory of Water Pollution Control and Resource Reuse, School of Environmental Science and Engineering, Shandong University, Jinan 250100 China

*Corresponding author, e-mail: sduchemzhang@163.com

Received 8 Oct 2021, Accepted 3 Mar 2022
Available online 25 May 2022

ABSTRACT: To tackle the issue of environmental pollution caused by heavy metal ions, a novel malic acid modified activated carbon (denoted as MA-AC) from (the plant) *Phragmites australis* has been successfully prepared with high Ni^{2+} adsorption capacity (38.36 mg/g). The physical and chemical characteristics of MA-AC were evaluated by N_2 adsorption/desorption, Scanning Electron Microscope (SEM), Fourier Transform Infrared (FTIR), and X-ray Photoelectron Spectroscopy (XPS). The results indicated that the MA-AC has more microporous structures and more oxygen bearing functional groups than the unmodified AC (denoted as AC). The Ni^{2+} adsorption behaviors of the adsorbents were investigated by batch experiments, which indicated that the MA-AC showed 38% higher Ni^{2+} adsorption capacity than the unmodified AC. The adsorption isotherms and the kinetics of the absorbents agreed well with the Langmuir model and the pseudo-second-order model. The Ni^{2+} adsorption mechanisms of MA-AC were investigated by FTIR and XPS analyses. The results from the analyses indicated that the enhanced surface adsorption of Ni^{2+} on MA-AC are attributed to the chemistry between the Ni^{2+} and the oxygen-containing functional groups on the surface.

KEYWORDS: malic acid, activated carbon, Ni^{2+} adsorption

INTRODUCTION

Ni(II) is widely used in the steel, battery, electroplating, and petrochemical industries, and the discharged Ni(II) in the aquatic environment can be consumed by human beings and animals. Ni(II) is considered a toxic heavy metal that can cause dermatitis, vomiting, cancers of the respiratory tract, and serious environmental pollutions. Therefore, the removal of heavy metal ions from waste water is a major issue that we should address. Among various technologies, the adsorption technique has proven to be an effective method [1, 2], leading to the development of highly efficient, cost effective, and eco-friendly adsorbents. Activated carbons (ACs) are promising adsorbents in the removal of heavy metal ions because of their highly developed porosity, high specific surface area, and excellent adsorption capacity [3].

In recent years, great efforts have been focused on the preparation of ACs from biomasses, which has emerged as a powerful solution. *Phragmites Australis* (PA) is a perennial wetland plant that can be found in many places: deltas, marshes, lake belts, river edges, roadsides, and ditches. A large number of stalks and leaves would rot off if they are not harvested at the end of the growing season. Hundreds of thousand tons of reeds are discarded or burned as fuel each year, leading to wastes of resources and environmental pollutions. PA contains lots of fibers and exhibits a multilayered structure. It is an attractive option because it has enhanced adsorption properties due to fibrous porous carbon, and it is cheap [4]. However, because the adsorption process is a surface reaction; and to obtain higher adsorption capability, several modification techniques have been made to optimize the AC surface [5–7] and, hence, enhances the adsorption performance. Therefore, the development of surface modified ACs continues to be an enormous challenge.

Finding cheap and non-toxic modified reagents is also a particular challenge in the preparation of ACs. Low-cost, non-poisonous malic acid (MA) is a carboxylic acid with two carboxyl groups and one hydroxyl group which could enhance carboxylic, lactone, or hydroxy functional groups on the surface of ACs. Phosphoric acid (H_3PO_4) can be transformed to polyphosphoric acid at high temperatures, and the polymeric species promote the polymerization reaction between the acid and organic matters. MA could initiate condensation reaction with phosphoric acid to form a phosphate ester, promoting the porosity and increasing the surface oxygen-containing functional groups of ACs [8]. The malic acid modified activated carbon (MA-AC) from *Phragmites australis* has been successfully prepared for the first time, and it showed obviously better adsorption performance of Ni^{2+} in solution than unmodified AC (denoted as AC). The enhanced surface adsorption of Ni^{2+} on MA-AC is attributed to the chemistry between the Ni(II) and oxygen-containing functional groups on the surface.

The main objectives of this study were to inves-

tigate the performance of MA-AC by batch Ni^{2+} adsorption experiments and to explore the properties of MA-AC as an adsorbent. The physicochemical properties of the MA-AC are evaluated by N_2 adsorption/desorption, SEM, FTIR, and XPS.

MATERIALS AND METHODS

Materials

All chemicals were of analytical grade, and all solutions were prepared with distilled water. *Phragmites australis* (PA) was obtained from a wetland located in Shandong Province, China. To remove dust and impurities, the PA was washed several times with distilled water, then dried at 105 °C for 24 h and crushed into pieces of approximately 0.45–1.0 mm.

Experimental procedure

The dried PA (1.0 g) was soaked in H_3PO_4-MA solution (0.02 mol H_3PO_4 and 0.01 mol MA) and then placed at room temperature for 12 hours. The mixture was carbonized at 450 °C for 1 h in a N_2 atmosphere. After cooling to room temperature, MA-ACs were washed with distilled water until the pH was close to 7.0 and then filtered and dried at 105 °C. Finally, the dried carbons were ground into flour and sieved to 100/160 meshes by standard sieves (Model Φ200). The unmodified ACs were prepared by the aforementioned method without adding MA.

Analytical methods

The pore structure and surface area of the ACs were determined by N_2 adsorption/desorption at 77 k using a surface area analyzer (Quantachrome Corporation, USA). The surface morphology of the ACs was detected using a SEM (JEOL, JSM 7600F, Japan). Functional groups of the carbons were analyzed with a FTIR (Fourier-380FTIR, USA) in the scanning wavenumber of 400–4000 cm^{-1}. The surface binding state and the elemental species of MA-ACs before and after Ni^{2+} adsorption were analyzed by XPS. The measurements were performed by a spectrometer (ESCALAB 250) with AL Ka irradiation (1486.8 eV of photons) as X-ray source.

Metal ions adsorption studies

The adsorption experiments were carried out by adding 40 mg MA-AC to 50 ml $NiCl_2$ solution (20 mg/l) at 25 ± 2 °C. The pH values of the $NiCl_2$ solutions were adjusted from 2 to 8 by NaOH (0.10 mol/l) and HCl (0.10 mol/l). The effect of ionic strength on the adsorption was also investigated by adding NaCl.

Adsorption isotherm experiments were evaluated between 20 and 80 mg/ml. The residual concentrations of Ni^{2+} were measured using a UV-vis spectrophotometer (UV-754, Shanghai) at 530 nm [9]. The amounts of Ni^{2+} adsorbed on the ACs, Q_e (mg/g), were calculated using the following equation:

$$Q_e = (C_0 - C_e)V/W,$$

where C_0 and C_e are the initial and the equilibrium concentrations of the Ni^{2+} in the aqueous solution (mg/l), respectively; V is the volume (l) of the solution; and W is the mass (g) of the adsorbent used.

The Ni^{2+} adsorption isotherms of unmodified AC and MA-AC were fitted by: Langmuir model: $Q_e = Q_{\max}K_L C_e/(1 + K_L C_e)$ and Freundlich model: $Q_e = K_F C_e^{1/n}$ [10], where Q_e is the equilibrium absorption capacity of Ni(II) (mg/g); C_e is the equilibrium concentration of Ni(II) solution (mg/l); K_L is the Langmuir constant (l/mg); $Q_{\max}$ is the monolayer adsorption capacity (mg/g); and K_F is the Freundlich affinity coefficient $(mg/g(l/mg)^{1/n}$; n is the Freundlich linearity index.

RESULTS AND DISCUSSION

Structure characterization

The surface area of adsorbents has a certain effect on the adsorption of Ni^{2+} in the adsorption process. Hence, we first measured the surface area of unmodified ACs and MA-ACs by Brunauer-Emmett-Teller (BET) measurements (Fig. 1). The results showed that both the unmodified AC and the MA-AC exhibit arrow knees at low pressure region, suggesting the presence of micropore structure. In addition, the hysteresis loops at high pressure indicated the existence of well-developed mesopores. Table S1 shows the parameters of the surface area and the pore volume of unmodified AC and MA-AC, which exhibits that the MA-AC had larger S_{BET} and S_{mic} than the unmodified AC, and suggesting more adsorption sites provided by former than the later. Both the S_{mic}/S_{BET} values of the MA-AC and the unmodified AC were lower than 15%, and the $V_{mic/Vtot}$ value was under 7%, indicating the mesoporous structure distribution in their pore structure (2–50 nm).

To study the morphologies of the unmodified AC and the MA-AC, SEM was measured (Fig. 2), which indicated that there were many irregular pores with cotton-shaped appearance on the adsorbents surface. The pores of the MA-AC were more intensive than those of the unmodified AC, which possibly was due to the fact that the introduction of malic acid had a great influence on pore size distribution.

Surface chemical characteristics of adsorbents

The FTIR spectra of MA-AC and unmodified AC were also measured (Fig. 3A), revealing the existence of —OH, C=O (carboxyl or lactone groups), and C—O groups in the samples. The very broad peak at 3400 cm^{-1} was due to the stretching vibration of —OH in the carboxyl and phenol groups. The peaks at 1585 cm^{-1} and 1700 cm^{-1} were assigned to stretching

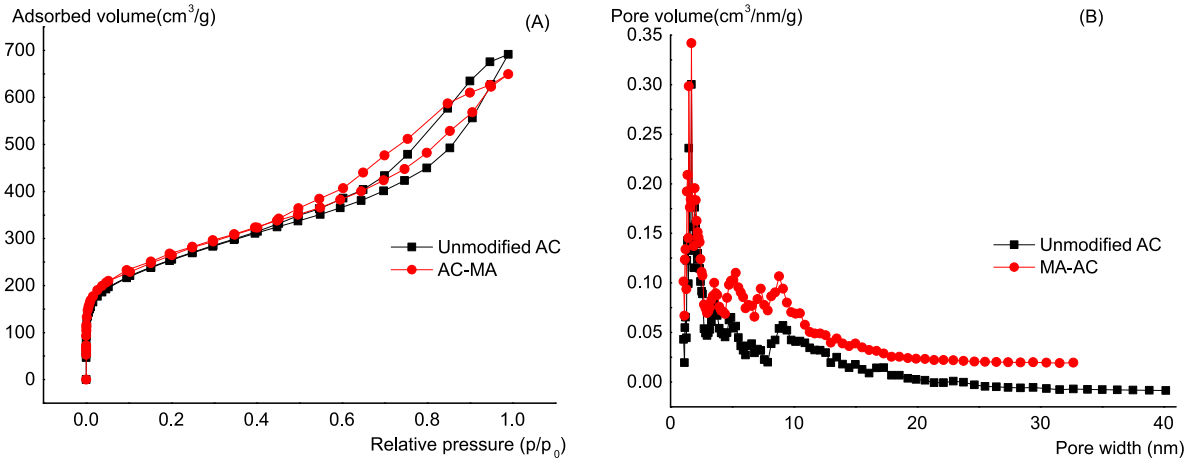

Fig. 1 N_2 adsorption/desorption isotherms (A) and pore size distributions (B) of unmodified AC and MA-AC.

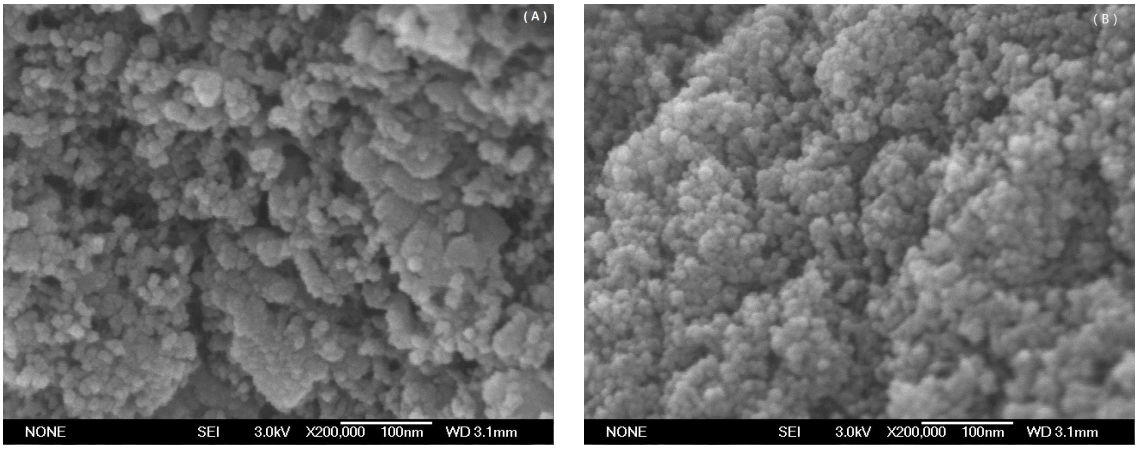

Fig. 2 SEM images of (A), unmodified AC and (B), MA-AC (magnification of A and B: 200 000).

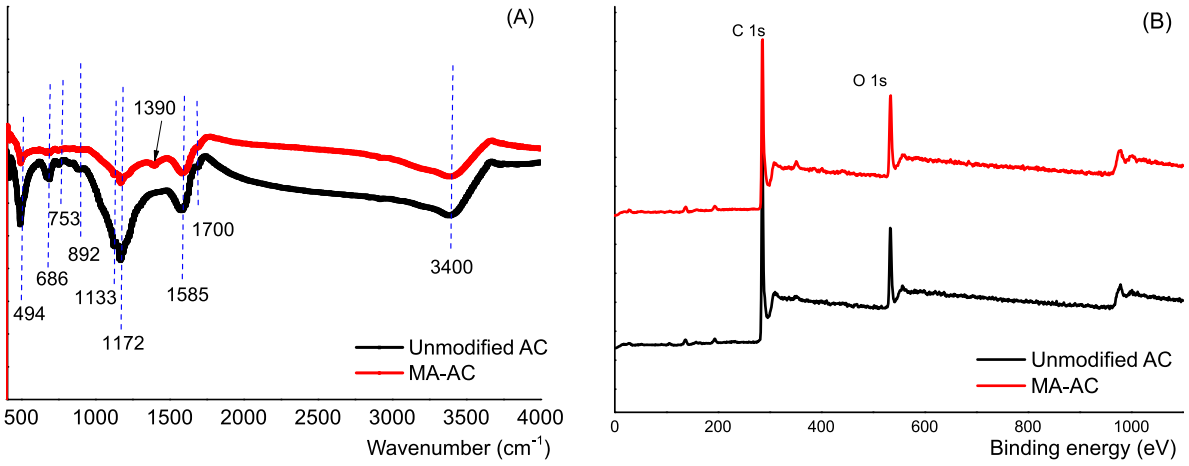

Fig. 3 FTIR spectra (A) and XPS spectra (B) of unmodified AC and MA-AC.

vibration of the C=O group. The peaks at 1133 cm^{-1} and 1172 cm^{-1} could be attributed to C—O groups. The peaks at 494, 686, 753, and 892 cm^{-1} were due to C—H chemical bonds [11]. The peak of MA-AC at 1390 cm^{-1} corresponded to C—O (lactone or phenolic hydroxyl groups) stretching vibration, which indicated that oxygen-containing functional groups increased during the modification process compared with the unmodified AC.

The XPS spectra were employed to identify the composition of the surface elements, as shown in Fig. 3B. The results revealed that C and O were the major elements on the surface of the ACs. The percentages of O/C calculated by the area-simulating curve on the surface for the unmodified AC and the MA-AC were 57% and 66%, respectively. The higher O/C percentage for the MA-AC suggested that it contained more oxygen-containing functional groups than the unmodified AC, which was consistent with the FTIR spectra's results.

Adsorption performance

The adsorption isotherms of Ni^{2+} on unmodified AC and MA-AC were fitted by the Langmuir model and the Freundlich model. The fitting curve was shown in Fig. 4A, and the adsorption isotherm constants were listed in Table S2. The adsorption isotherms of both unmodified AC and MA-AC matched the Langmuir model. The correlation coefficient (R^2) of the Langmuir model (Fig. 4C) was greater than 0.99, which demonstrated the monomolecular layer adsorption theory on the adsorbent surface, suggesting that only one Ni^{2+} ion was adsorbed per one site of adsorbent surface. The essential characteristics of Langmuir isotherm can be expressed according to equilibrium parameter R_L, which can judge the adsorption ability of the adsorbent. Since the R_L values of the unmodified AC and the MA-AC lied in the range of zero and one, indicating their favorable adsorption of Ni^{2+} for all studied concentrations.

Meanwhile, the Freundlich isotherm model (Fig. 4D) showed that the $1/n$ values for both unmodified AC and MA-AC were lower than 1, also suggesting the favorable adsorption of Ni^{2+} on them [12]. In addition, the adsorption strength constant (K_F) of the MA-AC was larger than that of the unmodified AC, indicating the stronger adsorption capacity of MA-AC. Both the maximum adsorption capacities (Q_m) obtained from Langmuir isotherm and the equilibrium absorption capacity (Q_e) illustrated the stronger adsorption capacity of the MA-AC than that of the unmodified AC. The experimental results of adsorption kinetics were illustrated in Fig. 4B. The adsorption capacity of the unmodified AC and the MA-AC increased sharply in the first one hour, and then the increases were slow down with time. At the beginning of the adsorption process, the rapidly increased adsorption capacity was due to the high concentration of Ni^{2+}. As the process continued, the concentration of Ni^{2+} ions in the solution decreased, and the adsorption sites on the surface of the adsorbents also decreased, resulting in the slower increase in adsorption capacity. Obviously, the adsorption capacity of Ni^{2+} on the MA-AC surface was much higher than that on the unmodified AC.

Two kinetic models, pseudo-first-order and pseudo-second-order, were applied to analyze the adsorption process of the unmodified AC and the MA-AC, and the results were displayed in Table S3. The evident gap between $Q_{e,cal}$ and $Q_{e,exp}$ illustrated that the Ni(II) adsorption processes on the unmodified AC and the MA-AC were not a first order reaction. Table S3 shows that the $Q_{e,cal}$ values calculated from pseudo-second-order kinetic equation agreed well with the experimental data ($Q_{e,exp}$). The higher correlation coefficients R^2 (Fig. 4E,F) (0.9999 for unmodified AC and 1.000 for MA-AC) indicated that the Ni^{2+} adsorption on the adsorbent was consistent with pseudo second-order reaction. The adsorption reactions involved complexation, chelation and valence forces through sharing or exchange of electrons between the adsorbent and the adsorbate [13]. Similar experimental results showed that there were perfectly agreeable between the pseudo-second-order kinetic model and the equilibrium data in aqueous solution [11]. The perfect fit with the pseudo-second-order kinetic model indicated that chemical adsorption had an important role on the rate control step of Ni^{2+} adsorption.

Effects of pH and ionic strength

Since the pH value of the solution also has a great effect on the adsorption process, the adsorption of Ni^{2+} in different pH solutions was carried out. The Ni^{2+} appears as different species in solution with different pH values, and there are five species: Ni^{2+}, $Ni(OH)^+$, $Ni(OH)_2^0$, $Ni(OH)_3^-$, and $Ni(OH)_4^{2-}$ owing to the fact that Ni^{2+} can combine with OH— by complexation at high pH (pH > 8), we studied the adsorption of Ni^{2+} on the surface of the ACs in the pH range from 2.0–8.0 (Fig. 5A). The results indicated that the adsorption increased sharply in the initial pH range of 2.0–4.0, and then slowly at the pH 4.0–8.0. The lower adsorption amount of Ni^{2+} at a lower pH solution was related to the electrostatic repulsion of positive electricity on the same surface. On one hand, the electrostatic repulsion between Ni^{2+} and H^+ took place constantly on the surface of the adsorbents. On the other hand, the H^+ could also occupy the surface adsorption sites of the adsorbents. However, the dissociation degree of the acidic functional groups on the surface of the carbons improved with the increase of pH. The higher pH (4.0–8.0) promoted the adsorption by the electrostatic attraction between the negative functional groups and

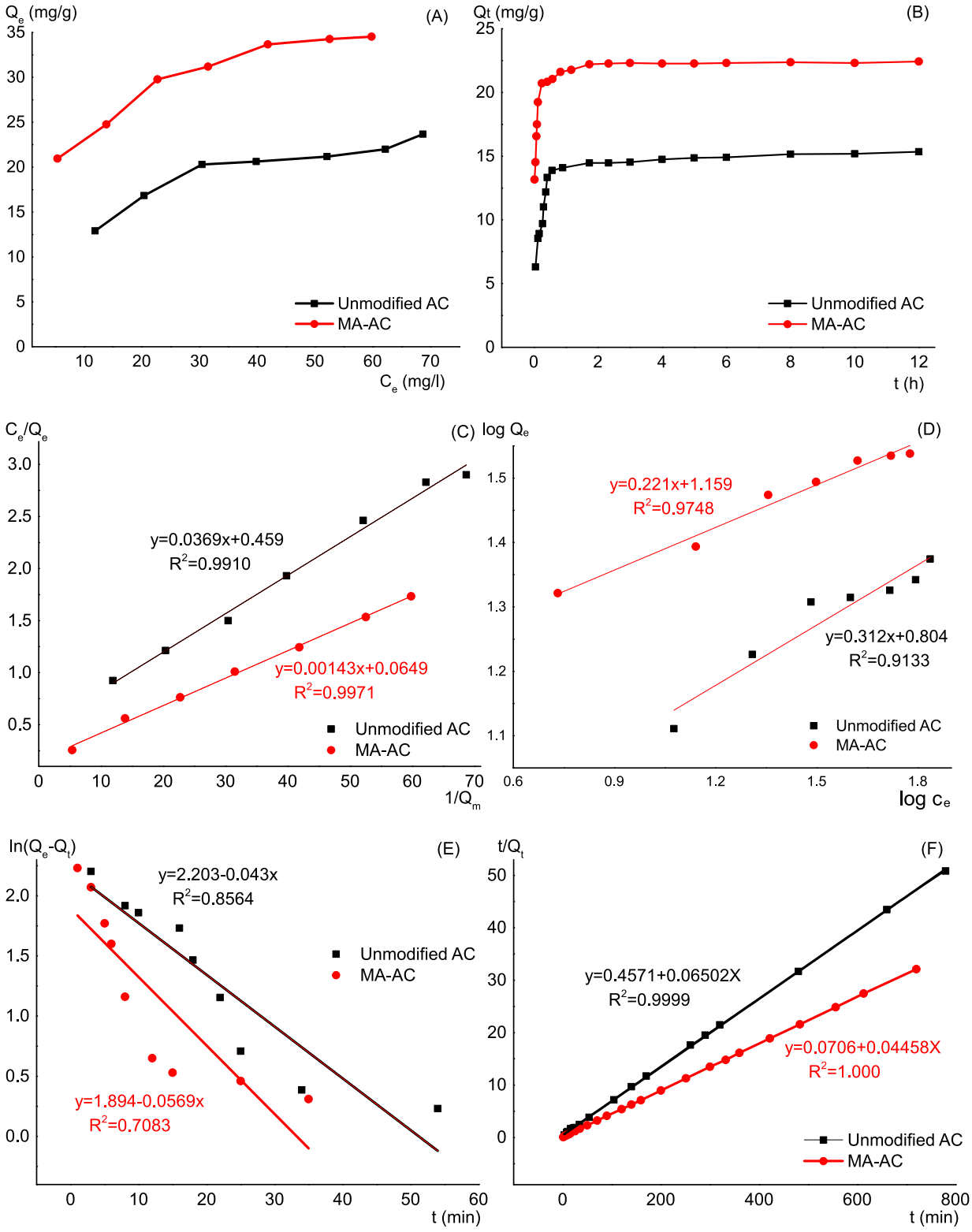

Fig. 4 Adsorption isotherms (A) and adsorption kinetics (B) of Ni^{2+} on unmodified AC and MA-AC; the linear plots of the Langmuir model (C), the linear plots of the Freundlich model (D); the linear plots of the pseudo-first-order model (E); and the linear plots of the pseudo-second-order model (F) (dosage = 40 mg/50 ml, temperature = 25 ± 1 °C, pH = 6.00 ± 1. (A): C_0 = 20–80 mg/l, (B): C_0 = 20 mg/l).

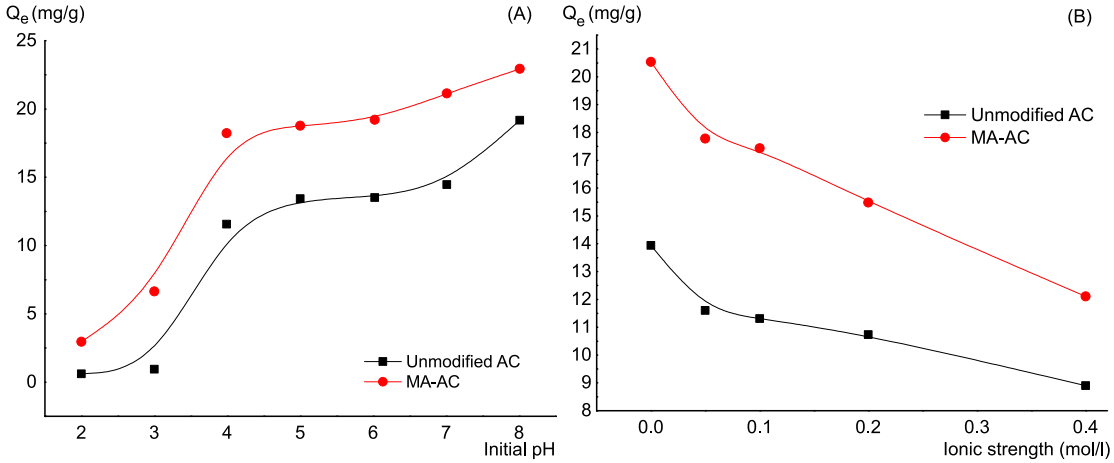

Fig. 5 Effects of initial pH (A) and ion strength (B) on the adsorption of Ni^{2+} on unmodified AC and MA-AC. (dosage = 40 mg/50 ml, temperature = 25 ± 1 °C, C_0 = 20 mg/l: (A), pH = 2.00–8.00; (B), pH = 6.00 ± 1.

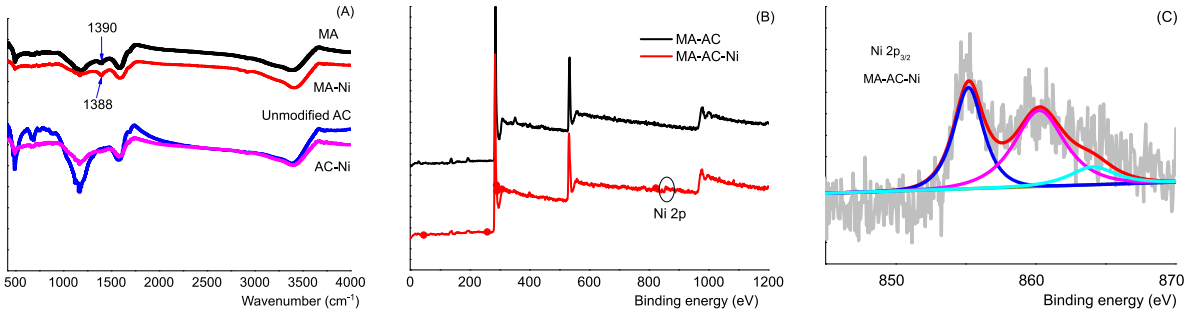

Fig. 6 FTIR spectra for Ni(II) adsorption, (A); and XPS survey spectra for Ni(II) adsorption, (B); Ni $2p_{3/2}$ XPS spectral of MA-AC, (C).

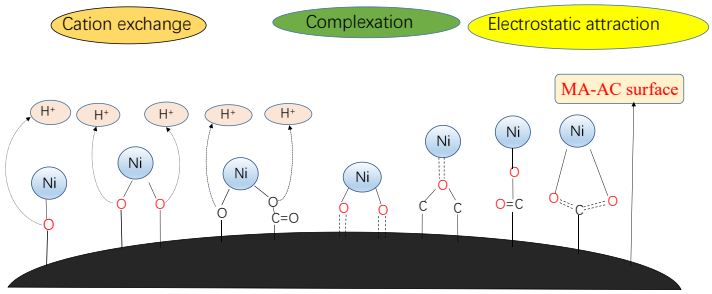

Fig. 7 Adsorption mechanism.

Table 1 Maximum Ni(II) adsorption capacity of different ACs by different modifying agents.

Carbon precursor	Modifying agent	Q_{max} (mg/g)	Reference
Commercial GAC (F 400)		3.12	[18]
Ligin	KOH	15.90	[19]
Commercial AC		2.90	[20]
Wood chips (pine and spruce)	$ZnCL_2$	18.20	[20]
Fireweed	H_2SO_4	2.97	[21]
Fireweed	H_2SO_4+NH_3	10.12	[21]
Phenolic resin	Fe_2O_3	13.83	[22]
Sawdust	1-(2-pyridylazo)-2-naphthol (PAN)	22.13	[23]
Phragmites australis	H_3PO_4	27.78	This work
Phragmites australis	H_3PO_4 + malic	38.36	This work

the Ni^{2+}. Accordingly, the adsorptions of Ni^{2+} on the unmodified AC and the MA-AC in the tested pH range were accompanied by notable proton releases, indicating the significant role of the cation exchange mechanism [14]. The adsorption curve of Ni^{2+} on the MA-AC was above that on the unmodified AC, indicating that the adsorption capacity of Ni^{2+} on the MA-AC was higher than that on the unmodified AC. Therefore, the higher adsorption capacity of Ni^{2+} on the MA-AC was attributed to its higher number of oxygen-containing functional groups than the unmodified AC.

It is worth noting that the salts in the wastewater also have great effects on the adsorption of heavy metals. To evaluate the effect of ionic strength on the adsorption of Ni^{2+}, adsorption experiments were carried out by adding NaCl at five different concentrations, as shown in Fig. 5B. The results indicated that the adsorption capacity of the ACs decreased distinctly with the increasing ionic strength from 0 to 0.4 M. This may be due to the adsorption of two different surface complexes. The adsorbed ions or molecules can form covalent bonds with the AC by ion exchange and electrostatic interactions in the inner sphere surface complexes; while their primary interaction force contains ion exchange, electrostatic attraction, and hydrogen bonding in the outer sphere surface complexes. There was competition between Na^+ and Ni^{2+} for adsorption sites on the adsorbent surface. On one hand, the increase of ionic strength could reduce the adsorption site for Ni^{2+}; on the other hand, the electrostatic interactions between Ni^{2+} and the deprotonated carboxyl groups could be decreased because many Na^+ ions partially neutralized the negative surface charges of the carbons and further accumulated in the vicinity of the adsorbent surfaces. Based on above analysis, the effect of ionic strength on Ni^{2+} adsorption on the MA-AC was higher than that on the unmodified AC, owing to the higher number of oxygen-containing functional groups in the MA-AC.

Adsorption mechanism

According to the above experimental analysis, the MA-AC had more surface oxygen-containing functional groups and much larger Ni(II) adsorption capacity than the unmodified AC. This indicated that surface chemistry of the ACs played an important role in Ni(II) adsorption. To further explore the adsorption mechanisms of Ni^{2+}, FTIR and XPS of MA-AC before and after Ni(II) adsorption were analyzed.

The FTIR spectra of the adsorbents before and after Ni(II) adsorption were shown in Fig. 6A. All of the peaks and their intensities became shifted and weaker after Ni(II) adsorption, indicating that surface functional groups of the ACs had participated in chemical reactions with Ni(II). XPS was tested to confirm the combination types between surface functional groups and Ni(II), as shown in Fig. 6B. The new Ni 2p peak appeared at 855 eV and 861 eV (Ni $2p_{3/2}$, Fig. 6C) of MA-AC-Ni indicating the formed chemical bonding between Ni^{2+} and oxygen functional groups (such as R—O, —COO, C—O—C) [15].

The C 1s and O 1s peaks of the MA-AC before and after Ni(II) adsorption were shown in Fig. S1, which displays that the C 1s spectrum could be fitted to three curves from respective groups: C—C or C—H at 283.65–284.81 eV; C—O in alcohol, phenol, or ether at 285.53–286.59 eV; and O=C—O or C=O at 288.15–289.26 eV [16]. The O 1s spectrum should be fitted to three peaks: C=O at 530.3–531.4 eV; C—OH or C—O—C at 532.26–533.26 eV; and chemisorbed oxygen (carboxylic groups) or water at 535.20–535.68 eV [17]. The fitting parameters of C 1s and O 1s curves were shown in Table S4. The C 1s spectrum shows that the binding energy (BE) of MA-AC after Ni(II) adsorption had fallen slightly, this indicated that Ni(II) and surface functional groups of MA-AC underwent chemical reactions. Peak III showed that more carboxylic groups of MA-AC decreased obviously after the adsorption of Ni^{2+}, hence indicating the forming of carbonyl-Ni complexes by ion exchange action between Ni^{2+} and H^+. The peak area ratios of C—O, C—O—C, and O=C—O for MA-AC-Ni showed a falling-off, which suggested that the complexation of Ni(II) and oxygen-containing functional groups was a critical way to remove Ni(II). In addition, the percentage of O/C for MA-AC decreased from 66% to 59%, which indicated that surface oxygen containing groups had participated in the Ni(II) adsorption.

The comparison of the maximum Ni^{2+} adsorption capacity of different ACs with different modifying agents was shown in Table 1. MA-AC exhibited higher Ni^{2+} adsorption capacity than other ACs, which indicated that MA-AC was a promising adsorbent for Ni^{2+} in aqueous solutions.

CONCLUSION

The preparation of ACs from PA as an efficient adsorbent for Ni^{2+} has been successfully achieved. Modification with malic acid of the AC created MA-AC that enhanced its adsorption for Ni^{2+}. The maximum adsorption capacity of Ni^{2+} on MA-AC was 38.36 mg/g, which was 38% higher than that on unmodified AC (27.78 mg/g). The effects of concentration, ionic strength, and pH values on the adsorption for Ni^{2+} on MA-AC were also discussed. The Ni^{2+} adsorption ability of AC improved with increasing initial pH; however, the ability decreased with increasing ionic strength (NaCl). The equilibrium data were well fitted with the Langmuir isotherm model and pseudo-second-order kinetic model. The MA-AC had a larger surface area, more microporous structures, and higher number of surface oxygen-containing functional groups than the unmodified AC. The results of XPS and FTIR analyses confirmed that the surface chemistry of MA-AC played

an important role on the Ni(II) adsorption. The main Ni^{2+} adsorption mechanisms of the MA-AC included cation exchange, surface complexation, and electrostatic attraction, as shown in Fig. 7. The study can shed new light on the novel adsorption materials in their applications to the environmental crisis.

Appendix A. Supplementary data

Supplementary data associated with this article can be found at http://dx.doi.org/10.2306/scienceasia1513-1874.2022.077.

Acknowledgements: This work was supported by the National Natural Science Foundation of China (No. 51878388), the Shandong Provincial Natural Science Foundation (No. ZR2018QEE006), and the Young Innovative Talents Introduction & Cultivation Program for Colleges and Universities of Shandong Province: Innovative Research Team on Optoelectronic Functional Materials.

REFERENCES

1. Krasnova TA, Belyaeva OV, Gorelkina AK, Timoshchuk IV, Golubeva NS (2020) Trichloroethylene adsorption from aqueous solutions by activated. *Carbon Lett* **30**, 281–287.
2. Rawinipa S, Jakkapan P (2021) Development of chitosan beads as an oil adsorbent and its application in household grease traps. *ScienceAsia* **47**, 330–339.
3. Aniagor CO, Elshkankery M, Fletcher AJ, Morsy OM, Abdel-Halim ES, Hashem A (2021) Equilibrium and kinetic modelling of aqueous cadmium ion and activated carbon adsorption system. *Water Sci Technol* **6**, 95–104.
4. Guo Z, Jian Z, Hai L (2016) Ultra-high Rhodamine B adsorption capacities from an aqueous solution by activated carbon derived from *Phragmites australis* doped with organic acid by phosphoric acid activation. *Rsc Adv* **6**, 40818–40827.
5. Rahayu S, Kurniawidi DW, A'Yun Q, Alaa S (2021) The effect of CaO doping in activated carbon composite as a heavy metal adsorbent in water. *IOP Conf Ser: Earth Environ Sci* **718**, ID 012063.
6. Rajumon R, Aravind SP, Bhuvaneshwari S, Ranjitha J, Mohanraj P (2020) Removal of cadmium heavy metal ions from wastewater by electrosorption using modified activated carbon felt electrodes. *Water Sci Technol* **82**, 1430–1444.
7. Nieto-Delgado C, Gutiérrez-Martínez J, Rangel-Méndez J (2019) Modified activated carbon with interconnected fibrils of iron-oxyhydroxides using Mn^{2+} as morphology regulator, for a superior arsenic removal from water. *J Environ Sci* **76**, 406–417.
8. Liu H, Wang X, Zhai G, Zhang J, Zhang C, Bao N, Cheng C (2012) Preparation of activated carbon from lotus stalks with the mixture of phosphoric acid and pentaerythritol impregnation and its application for Ni(II) sorption. *Chem Eng* **209**, 155–162.
9. Huang LH, Sun YY, Tao Y, Li L (2011) Adsorption behavior of Ni(II) on lotus stalks derived active carbon by phosphoric acid activation. *Desalination* **268**, 12–19.
10. Guo Z, Fan J, Zhang J, Kang Y, Liu H, Jiang L, Zhang CL (2016) Sorption heavy ions by carbons with well-developed microporosity and amino groups derived from *Phragmites australis* by ammonium phosphate activation. *J Taiwan Inst Chem Eng* **58**, 290–296.
11. Shang Z, Hu Z, Huang L, Guo Z, Liu H, Zhang CL (2020) Removal of amoxicillin from aqueous solution by zinc acetate modified activated carbon derived from reed. *Adv Powder Technol* **368**, 178–189.
12. Hai L, Wei N, Cheng P, Zhang J, Yan W, Zhang CL (2013) Evaluation of animal hairs-based activated carbon for sorption of norfloxacin and acetaminophen by comparing with cattail fiber-based activated carbon. *J Anal Appl Pyrol* **101**, 156–165.
13. Wu Q, Ye X, Lv Y, Pei R, Liu M (2020) Lignin-based magnetic activated carbon for p-arsanilic acid removal: Applications and absorption mechanisms. *Chemosphere* **258**, ID 127276.
14. Luan L, Tang B, Ma S, Sun L, Xu W, Wang A, Niu Y (2021) Removal of aqueous Zn(II) and Ni(II) by Schiff base functionalized PAMAM dendrimer/silica hybrid materials. *J Mol Liq* **330**, ID 115634.
15. Liu H, Zhang J, Ngo HH, Guo W, Wu H, Cheng C, Guo Z, Zhang C (2015) Carbohydrate-based activated carbon with high surface acidity and basicity for nickel removal from synthetic wastewater. *Rsc Adv* **5**, 52048–52056.
16. Blanco E, Sepulveda C, Cruces K, García-Fierro JL, Ghampson IT, Escalona N (2020) Conversion of guaiacol over metal carbides supported on activated carbon catalysts. *Catal Today* **356**, 376–383.
17. Zhang H, Li S, Jiao Y, Iojoiu E, Costa PD, Galvez M, Chen Y (2019) Structure, surface and reactivity of activated carbon: From model soot to bio diesel soot. *Fuel* **257**, ID 116038.
18. Nguyen T, Ngo HH, Guo WS, Zhang J, Nguyen TV (2013) Applicability of agricultural waste and by-products for adsorptive removal of heavy metals from wastewater. *Bioresour Technol* **148**, 574–585.
19. Gao Y, Yue Q, Gao B, Sun Y, Wang W, Li Q, Wang Y (2013) Preparation of high surface area-activated carbon from lignin of papermaking black liquor by KOH activation for Ni(II) adsorption. *Chem Eng J* **217**, 345–353.
20. Runtti H, Tuomikoski S, Kangas T, Lassi U, Kuokkanen T, Rämö J (2014) Chemically activated carbon residue from biomass gasification as a sorbent for iron(II), copper(II) and nickel(II) ions. *J Water Process Eng* **4**, 12–24.
21. Dwivedi AD, Dubey SP, Sillanpää M, Kwon Y-M, Lee C (2015) Distinct adsorption enhancement of bi-component metals (cobalt and nickel) by Fireweed-derived carbon compared to activated carbon: Incorporation of surface group distributions for increased efficiency. *Chem Eng* **281**, 713–723.
22. Lee CG, Lee S, Park JA, Park C, Lee SJ, Kim SB, An B, Yun ST, et al (2017) Removal of copper, nickel and chromium mixtures from metal plating wastewater by adsorption with modified carbon foam. *Chemosphere* **166**, 203–211.
23. Aia B, Mrj AJ (2021) Recovery of cadmium, lead and nickel from leach solutions of waste electrical and electronic equipment using activated carbon modified with 1-(2-pyridylazo)-2-naphthol. *Hydrometallurgy* **201**, ID 155070.

Appendix A. Supplementary data

Table S1 Surface areas and pore volume parameters of unmodified AC and MA-AC.

Sample	Unmodified AC	MA-AC
S_{BET} (m^2/g)	911	956
S_{mic} (m^2/g)	110	139
V_{mic} (cm^3/g)	0.05	0.06
V_{mes} (cm^3/g)	0.94	0.85
V_{tot} (cm^3/g)	0.99	0.91
D_p (nm)	4.33	3.81

Table S2 Langmuir and Freundlich isotherms parameters of unmodified AC and MA-AC for Ni(II) adsorption.

Sample	Langmuir isotherm				Freundlich isotherm		
	Q_m (mg/g)	K_L (l/mg)	R^2	R_L	K_F (mg/g(l/mg)$^{1/n}$)	$1/n$	R^2
Unmodified AC	27.78	0.078	0.9925	0.128–0.364	6.35	0.312	0.9277
MA-AC	38.36	0.166	0.9976	0.064–0.212	14.39	0.220	0.9790

Table S3 Kinetic parameters of the pseudo-first order and pseudo-second order models for the adsorption of Ni^{2+} on unmodified AC and MA-AC.

Sample	$Q_{e,exp}$ (mg/g)	Pseudo first-order			Pseudo second-order		
		K_1 (1/h)	$Q_{e,cal}$ (mg/g)	R^2	K_2 (mg(g/h))	$Q_{e,cal}$ (mg/g)	R^2
Unmodified AC	15.35	0.0430	9.0521	0.8564	0.555	15.38	0.9999
MA-AC	22.42	0.0569	6.6459	0.7083	1.689	22.43	1.0000

Table S4 Peak numbers and relative content of the surface functional groups determined by C 1s and O 1s spectra from XPS for MA-AC before and after Ni(II) adsorption.

Sample		Peak of C 1s spectrucm			Peak of O 1s spectrucm		
		Peak 1 C—C, C—H	Peak 2 C—O	Peak 3 O=C—O	Peak I O=C—	Peak II (C—O—C, C—OH)	Peak III (COOH, O)
MA-AC	BE (eV)	284.81	286.59	289.26	531.44	533.26	535.68
	RC (%)	65.77	21.59	12.65	18.22	64.56	17.22
MA-AC-Ni	BE (eV)	283.65	285.53	288.15	530.30	532.26	536.20
	RC (%)	67.48	20.30	12.44	33.32	63.62	3.06

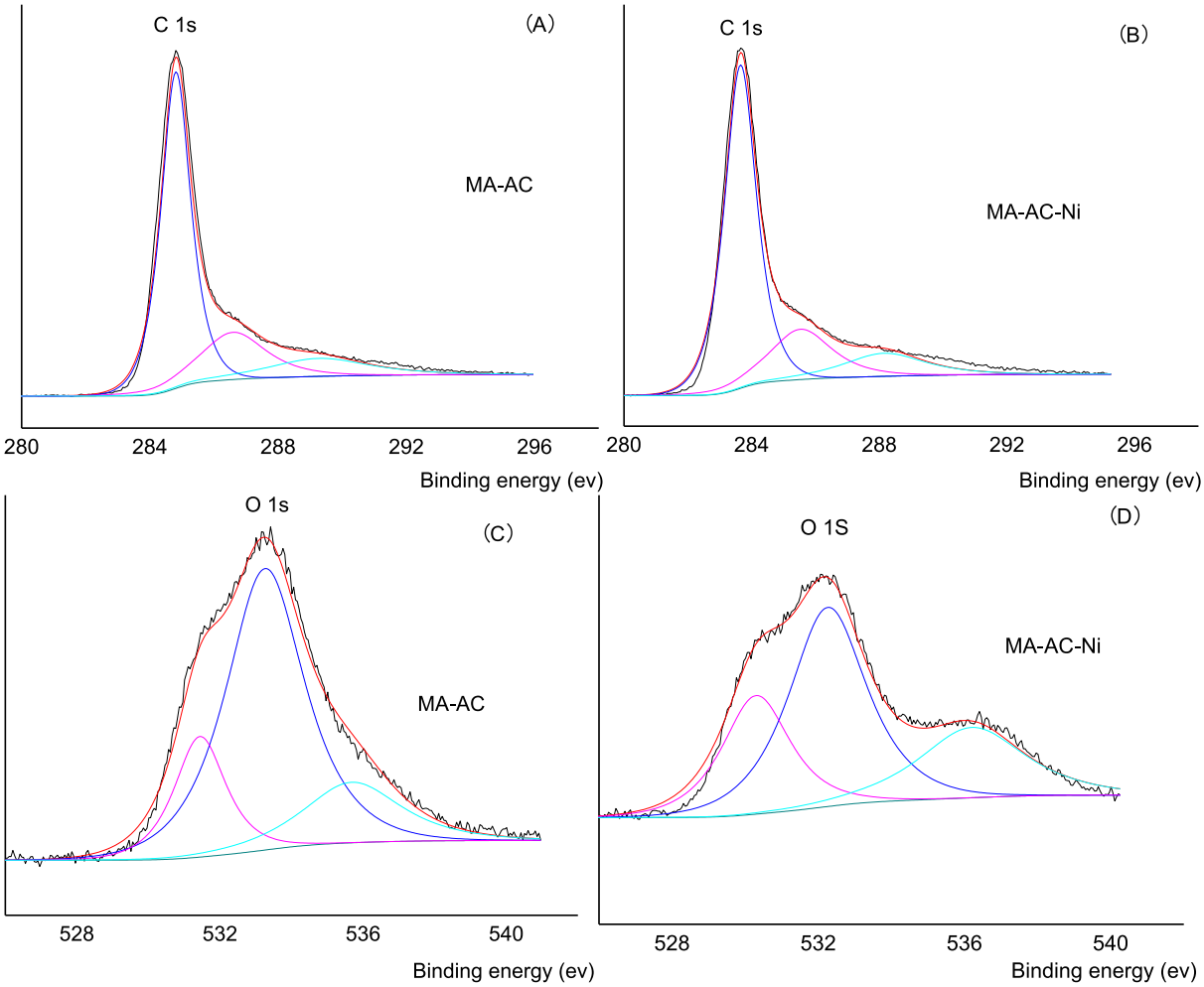

Fig. S1 XPS spectra for MA-AC before and after Ni(II) adsorption: C 1s (A and B) and O 1s (C and D).